Boron-content dependence of Fano resonances in p-type silicon

2003 J. Phys.: Condens. Matter 15 2923

(http://iopscience.iop.org/0953-8984/15/17/340)

INSTITUTE OF PHYSICS PUBLISHING JOURNAL OF PHYSICS: CONDENSED MATTER

J. Phys.: Condens. Matter **15** (2003) 2923–2931 PII: S0953-8984(03)56023-4

Boron-content dependence of Fano resonances in p-type silicon

R Gajić[1], D Braun[1], F Kuchar[1], A Golubović[2], R Korntner[3], H Löschner[3], J Butschke[4], R Springer[4] and F Letzkus[4]

[1] Department of Physics, Montanuniversität Leoben, Franz Josef Straße 18, 8700 Leoben, Austria
[2] Institute of Physics, PO Box 68, 11080 Belgrade, Serbia and Montenegro
[3] IMS Nanofabrication GmbH, Schreygasse 3, 1020 Wien, Austria
[4] Institut für Mikroelektronik Stuttgart—IMS Chips, Allmandring 30a, D-70569 Stuttgart, Germany

Received 13 November 2002, in final form 5 March 2003
Published 22 April 2003
Online at stacks.iop.org/JPhysCM/15/2923

Abstract

We present a study of Fano-type resonances in high quality boron-doped silicon as a function of boron content. The resonance (antiresonance) in the infrared absorption spectra occurs close to the $\vec{k} \approx 0$ optical phonon at 519 cm^{-1}. The interaction between the otherwise infrared-forbidden optical phonon and the continuum states of the acceptor was analysed based on a modified Fano model that involves the interaction of a discrete state with two continua.

1. Introduction

Fano interaction [1, 2] is a very frequent phenomenon in physics and appears in various systems from rare gases to semiconductors and superconductors. Generally, the Fano effect occurs when there is an interaction of a discrete state with a degenerate continuum of states. Due to quantum interference between transition probability amplitudes of discrete and continuum states, asymmetric line shapes appear. Its analysis allows us to get information on, and the basic interaction mechanism between, electronic and vibronic states in the solid. In p-type silicon Fano resonances have been observed in many experiments concerning infrared-absorption [3–8], photoconductivity [9–11] and Raman spectroscopy [12–15]. There, a resonant interaction takes place between the discrete state of the optical phonon and the hole continuum. The continuum could be identified as the hole continuum of the acceptor-to-band excitations, inter-valence transitions or free carrier absorption depending on experimental conditions. The purpose of this work is to investigate experimentally the role of the boron doping in silicon, to analyse the Fano profile on the basis of a modified Fano model, and to identify the dominating interaction mechanisms. In the experimental part infrared transmission and reflection measurements were performed on thin membranes and bulk crystals, respectively. In particular, the dependence on acceptor concentration was studied for the boron range

10^{18}–10^{19} cm^{-3} for the first time. The details of the Fano resonance observed around 519 cm^{-1} seems to be in quite good agreement with a modified Fano model with two continua.

2. Experimental details

The samples used were thin silicon membranes and bulk silicon crystals. Most of the data were taken on thin, heavily boron-doped membranes with a thickness of 2 μm. The overall size of the membrane samples was 40×40 mm^2 with a membrane size of 25×25 mm^2. All samples had well defined and homogeneous concentrations of boron in the range 5×10^{18}–2×10^{19} cm^{-3} [16]. We have not seen any trace of impurities, proving the high quality of the samples used. In further study [17] the emissivity of such membranes was determined with respect to their use as stencil masks for ion-projection lithography [18, 19]. The bulk crystals were grown by the float-zone technique and doped either with n- or p-type (Sb and B, respectively) to investigate also the dependence on the doping type. Infrared transmission (membranes) and reflection (bulk crystals) were measured at room temperature using a Bruker IFS 113v Fourier-transform spectrometer.

3. Results and discussion

As an example of our measurements we present in figure 1 the infrared spectra of the Si(B) membrane specimen with a doping concentration of 1.3×10^{19} cm^{-3}. The feature we were interested in is framed in figure 1(a) and then enlarged in figure 1(b). This tiny, hardly visible, structure with its peak transmittance over background of only 1% has, compared to its size, quite interesting physics behind it. A glance at the normalized absorbance depicted in figure 1(d) reveals a typical Fano profile. This is the characteristic feature of the interaction and mixing of a discrete state with a continuum [1]. Similar resonances were observed in the absorbance spectra of differently p-doped Si to those in Ga and Al-doped Si [6, 7]. The effect does not exist in n-doped Si [8] as is also clearly visible from our reflectance measurements on bulk crystal (figure 2). This figure shows the spectra of Sb-doped Si (n-type) compared with spectra of B-doped samples. The dopant concentrations were chosen to be similar to those in the thin Si membranes, in the range 10^{18}–10^{19} cm^{-3}. In addition, it is shown that the Fano dip due to an optical phonon disappears in the spectrum when holes are missing in the acceptor sites either by an increase of the sample temperature or by doping compensation [8]. This result identifies the acceptor-to-band transitions as significant for the process. The reason for the interaction with only the hole continuum concerns the shallow acceptor levels in Si, which are separated by energies comparable to phonons. Moreover, the coincidence of the antiresonance peak with the zone-centre optical phonon does not seems to be accidental as an additional peak at 764 cm^{-1} with a Fano profile at the energy corresponding to the difference appears between 2 $P_{3/2}$ and 1 $S_{3/2}$ plus the 519 cm^{-1} optical phonon [6]. In addition to the acceptor-to-band transitions, inter-valence transitions have also been suggested [7, 20] as possible partners in the interaction with the optical phonon.

According to [6] this effect in p-doped silicon is associated with the resonant interaction of two states:

(a) a discrete state $|\varphi\rangle$, represents the hole in its acceptor ground state G and one locally excited optical phonon, and
(b) the state $|\psi_{E'}\rangle$ with no phonons created and the hole is excited into the $p_{3/2}$ valence band.

Even a small electron–phonon interaction V_E in non-polar systems such as Si will produce a mixing of these states and a resonant feature in the spectrum provided that degeneracy exists.

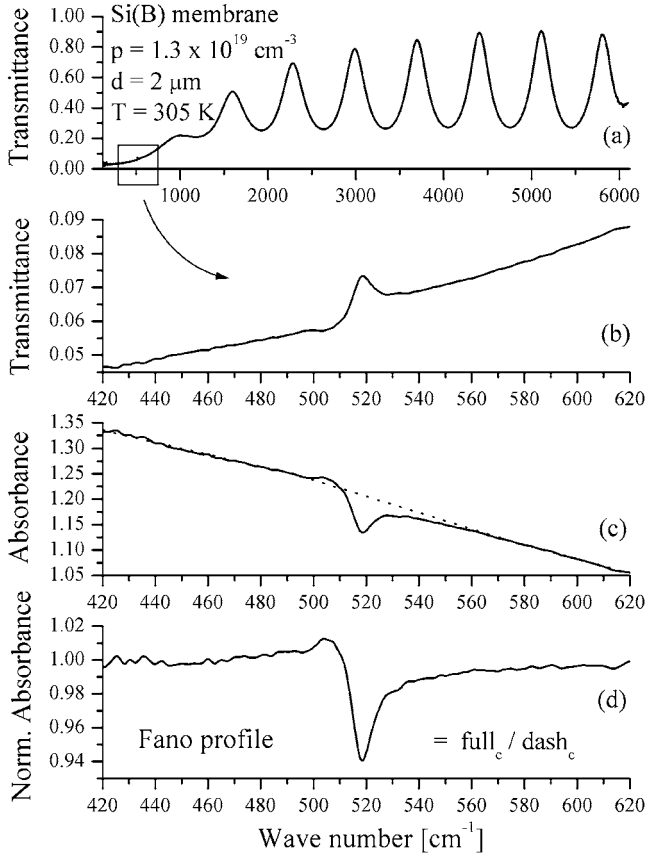

Figure 1. Infrared transmission spectrum of the sample with $p = 1.3 \times 10^{19}$ cm^{-3} and the Fano antiresonance peak in the absorbance ($-\log_{10} T$) at 519 cm^{-1}. (d) denotes a normalized absorbance from (c).

In other words there is a mixed state:

$$|\Psi_E\rangle = a|\varphi\rangle + \int \mathrm{d}E'\, b_{E'}|\psi_{E'}\rangle \tag{1}$$

where

$$|\varphi\rangle = |G, 1_{ph}\rangle \qquad \text{and} \qquad |\psi_{E'}\rangle = |\mathrm{p}_{3/2}, 0_{ph}\rangle. \tag{2}$$

The presence of acceptor impurities disrupt the symmetry of the crystal and allows the excitation of the otherwise infrared-forbidden optical phonon Γ'_{25} in silicon. As the acceptor states have some extension in real space, the portion of the q-space necessary for the construction of the impurity wavefunction has a small but non-zero volume. Therefore, the $\vec{q} \neq 0$ phonons are also allowed to participate in the process. Here we model the narrow phonon band around the $\vec{q} = 0$ phonon with the single phonon state $|\varphi\rangle$ broadened by a quasi-continuous phonon band VC as is depicted in figure 3. A similar model has been used [11] in the analysis of the photo-excitation spectra of chalcogen-doped silicon. Effectively, this means that there is an interaction of a discrete system with two continua. Fano's original analysis gives the ratio of the transition probability $|\langle\Psi_E|T|i\rangle|^2$, from the initial state to the perturbed continuum $|\Psi_E\rangle$

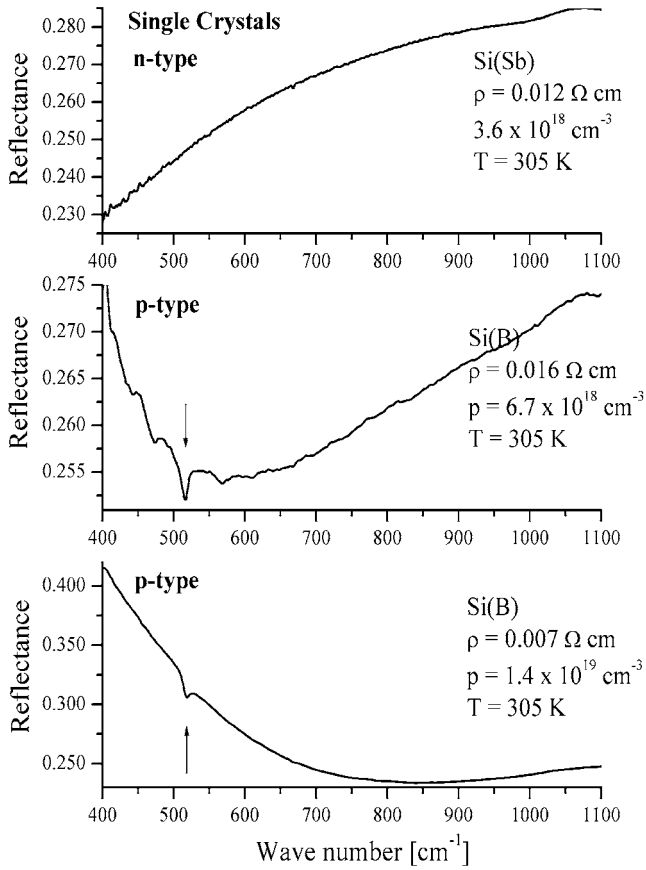

Figure 2. Reflectance spectra of p- and n-doped bulk Si. Fano peaks (arrows) are present only in the p-type Si.

(E is an eigenvalue of the full Hamiltonian H), to the probability $|\langle\psi_E|T|i\rangle|^2$ of transition to the unperturbed continuum by a single family of curves:

$$F(\varepsilon, q) = \frac{|\langle\Psi_E|T|i\rangle|^2}{|\langle\psi_E|T|i\rangle|^2} = \frac{(q+\varepsilon)^2}{1+\varepsilon^2} \tag{3}$$

where the energy ε and the parameter q are defined as:

$$q = \frac{\langle\Phi|T|i\rangle}{\pi V_E^*\langle\psi_E|T|i\rangle} \tag{4}$$

$$\varepsilon = -\cot\Delta = \frac{E - E_\varphi - \Sigma(E)}{\Gamma/2}, \qquad \Gamma = 2\pi|V_E|^2 \qquad \text{with} \qquad \langle\psi_E|H|\varphi\rangle = V_E \tag{5}$$

$|\Phi\rangle$ is the modified discrete state and $\Sigma(E)$ the frequency shift due to the electron–phonon interaction, respectively:

$$|\Phi\rangle = |\varphi\rangle + P\int \mathrm{d}E' \frac{V_{E'}|\psi_{E'}\rangle}{E - E'}, \qquad \Sigma(E) = P\int \mathrm{d}E' \frac{|V_{E'}|^2}{E - E'} \tag{6}$$

and T is the dipole transition operator.

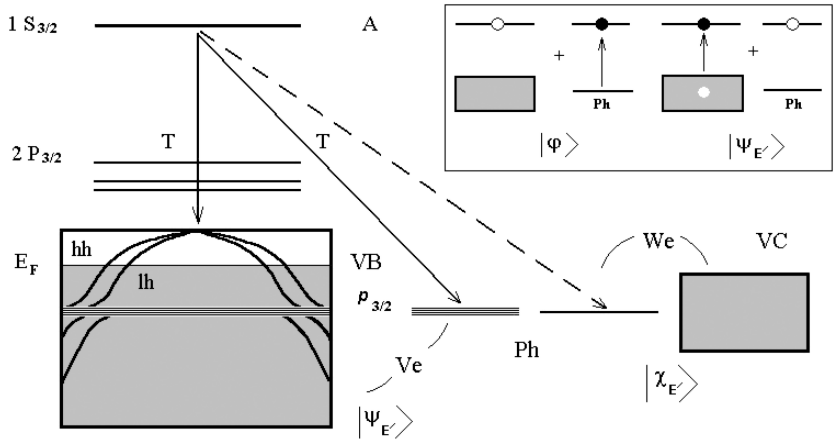

Figure 3. Scheme of interaction of holes with optical phonons. Here 1 $S_{3/2}$, 2 $P_{3/2}$, VB and VC denote the acceptor levels, the $p_{3/2}$ valence band with heavy holes (hh) and light holes (lh) and the virtual phonon continuum, respectively. The inset represents the states $|\varphi\rangle$ and $|\psi_{E'}\rangle$ defined in equation (2), whereas V_E and W_E are the matrix elements of electron–phonon and phonon–phonon interaction.

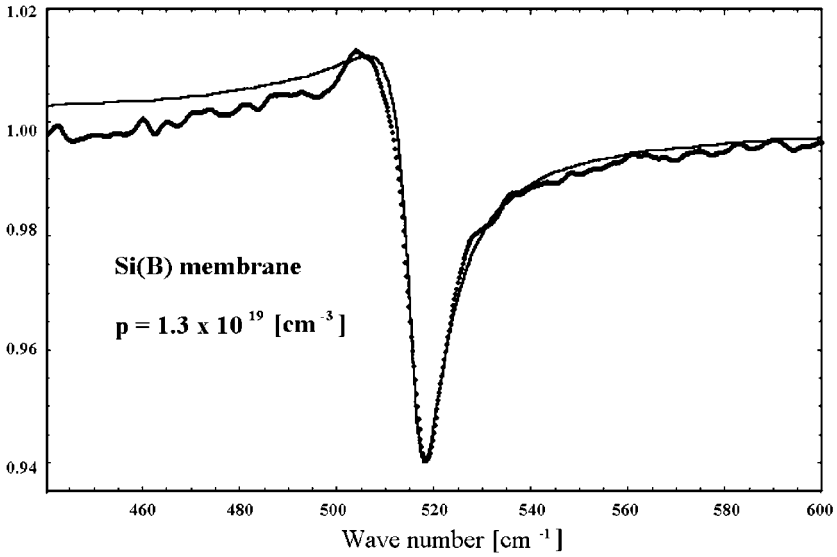

Figure 4. Fit of the normalized absorbance spectrum in figure 1(d) using the modified Fano model for the interaction of a discrete state with two continua. The full line denotes the fit.

$F(\varepsilon, q)$ is an asymmetric function of ε and equals zero at $\varepsilon = -q$. Looking at figure 1(d) we see that the normalized absorbance never drops to zero as is expected from (3). Therefore, we try to fit our experimental data using the following modified Fano function:

$$\bar{F}(\varepsilon, q) = a + bF(\varepsilon, q). \tag{7}$$

This function has already been used in many experiments from UV-absorption spectra of the rare gases [2] to Raman spectra of $BaTiO_3$ [21]. We have taken parameters a and b to be independent during the fit and it turned out that their sum was exactly 1. The result of the

fit is shown in figure 4. Checking the literature on Fano lines, we found few similar cases that concern the photoexcitation spectra of chalcogen-doped silicon [11] and photoemission spectra of atoms that include Auger recombination [22]. In all cases the authors used the modified Fano function (7) in the form:

$$\bar{F}(\varepsilon, q) = \frac{\Gamma_2}{\Gamma} + \frac{\Gamma_1}{\Gamma} F(\varepsilon, q), \qquad \Gamma = \Gamma_1 + \Gamma_2. \tag{8}$$

The effects described by (7) and (8) are connected with the interaction of one discrete state $|\varphi\rangle$ with two continua $|\psi_{E'}\rangle$ and $|\chi_{E'}\rangle$. Further detail of the Fano interaction and the derivation of (8) is given in the appendix. In our case we propose that $|\varphi\rangle$ represents the optical phonon, $|\psi_{E'}\rangle$ the valence continuum states and $|\chi_{E'}\rangle$ states in a virtual phonon continuum VC that interacts with the optical phonon as shown in figure 3. The main idea is to replace a quasi-continuous phonon band with a single optical phonon plus the virtual phononic continuum VC (figure 3), and then to apply the Fano model with two continua represented by equation (8) and explained in the appendix. It is worth emphasizing that in this case there is no transition from the initial state to the VC continuum (see relation (A.16)) but only to the discrete phonon state (dashed arrow in figure 3). As a result of the fitting procedure based on equation (8) we obtained the parameters presented in figure 5. It is interesting that parameters depending on electron–phonon interaction V_E show a nonlinear dependence on boron content. We defined $\Gamma_1 = 2\pi V_E^2$ that strictly holds for a true continuum with an infinite number of states as is implied by the δ function for the matrix element $\langle\psi_{E''}|H|\psi_{E'}\rangle = E'\delta(E' - E'')$. In practice, a quasi-continuum with a finite number of states per unit volume $\rho(E)$ gives $\Gamma_1 = 2\pi V_E^2 \rho(E)$. Taking $\rho(E_F)$ for $\rho(E)$ with the additional assumption of parabolic upper and lower (lh and hh) valence bands, one obtains [12]:

$$\rho(E) \cong \rho(E_F) = \text{constant} \frac{N_h - N_l}{E_F} \tag{9}$$

where N_h and N_l represent the number of carriers for heavy and light holes, respectively. Since

$$\frac{N_h}{N_l} = \left(\frac{m_h}{m_l}\right)^{3/2} \qquad \text{and} \qquad N_B = N_h + N_l \qquad \text{at } T = 300\ \text{K} \tag{10}$$

with the approximation of the Fermi–Dirac function $F_{1/2}(\xi)$ [23] for the moderate degeneracy:

$$F_{1/2}(\xi) = \frac{\sqrt{\pi}}{2} \frac{1}{0.25 + \mathrm{e}^{-\xi}}, \qquad -1 < \xi < 5,\ \xi = \frac{E_V - E_F}{kT} \tag{11}$$

one gets:

$$p = \frac{2}{\sqrt{\pi}} N_V F_{1/2}(\xi) \cong N_B \tag{12}$$

and the Fermi level as function of the boron concentration N_B. Therefore, Γ_1 is given as:

$$\Gamma_1 = \text{constant} \frac{N_B}{E_F(N_B)}. \tag{13}$$

In figure 5(a) the full line corresponds to the relation (13) and the dashed one to the complete degeneracy $\left(F_{1/2} = \frac{2}{3}\xi^{3/2}\right)$. Both models give a fairly good fit based on the electron–phonon interaction and relation (9) but for the highest boron concentration. A similar discrepancy has already been observed in Raman spectra of B-doped Si [12] at higher boron concentrations where the approximation (9) is no longer valid. In addition, in our case the hole states interacting with the phonons are below the Fermi level (see figure 3). On the other hand, Γ_2 and $\langle\Phi|T|i\rangle/\langle\psi_E|T|i\rangle$ (figures 5(b) and (d)), which represent an effective phonon–phonon interaction and do not depend on Γ_1, have a linear dependence on N_B. This can be explained

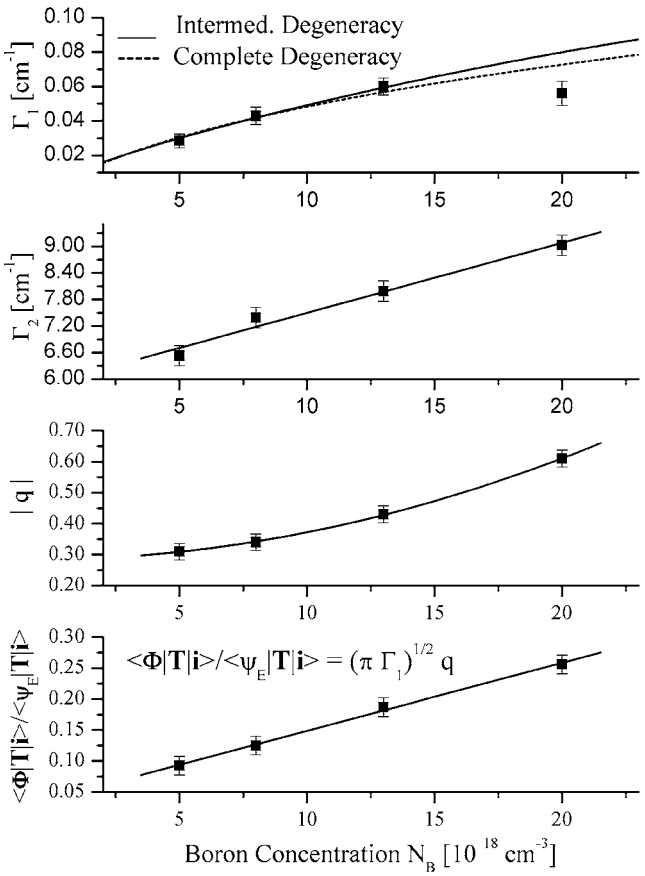

Figure 5. Parameters obtained using the fit according the two-continua Fano model. Parameters q and Γ_1 depend explicitly on the electron–phonon interaction.

as the phonon-defect impurity scattering with the collision frequency $\tau_s^{-1}(d)$ which is directly proportional to the defect concentration at room temperature [24, 25]. It is also worth emphasizing that the ratio $\Gamma_2/\Gamma_1 \geqslant 15$–$20$ indicating that the main scattering mechanism is due to the phonon-defect interaction within the quasi-continuous phonon band. In [6] the authors also took into account the phonon band and fit of the absorption line at 519 cm^{-1}. They treated phonons individually and allowed all of them to interact with the hole continuum. As a result they convolved the Fano function (3) with the phonon distribution function. In contrast we applied the two-continua Fano model that effectively allows the interaction of the $\vec{q} = 0$ phonon at 519 cm^{-1} with the hole continuum and the rest of the phonons separately. In all cases we obtained very good agreement between the experiment and the model.

4. Summary

In this paper we present room temperature infrared absorption spectra of boron-doped Si in the doping range 5×10^{18}–2×10^{19} cm^{-3}. The Fano line at 519 cm^{-1} is analysed and fitted according to the Fano model that involves interaction of a discrete state with two different continua. We found that it is necessary to take into account the phonon quasi-continuum band

around the $\vec{q} = 0$ optical phonon at 519 cm^{-1} to describe the process through an effective phonon–phonon interaction.

Acknowledgment

This work was supported by the Bundesministerium BMVIT Austria, the project no GZ 601. 593/2-V/A/5/2000.

Appendix

Here we closely follow the analysis of Fano [7] considering the interference between a single discrete state and two continua of states. Most of the formalism can be found in Fano's original paper although formula (8) was not derived explicitly. Equation (8) can also be obtained by the Green function method [11, 21]. For the case of the configurational interaction of a discrete state $|\varphi\rangle$ with states of two different continua $|\psi_{E'}\rangle$ and $|\chi_{E'}\rangle$, the eigenvectors are given by:

$$|\Psi_{nE}\rangle = a|\varphi\rangle + \int \mathrm{d}E' \,[b_{nE'}|\psi_{E'}\rangle + c_{nE'}|\chi_{E'}\rangle], \qquad n = 1, 2 \tag{A.1}$$

where n indicates that E is two-fold degenerate eigenvalue. In Fano's notation the matrix elements of a Hamiltonian H are given by:

$$\langle\varphi|H|\varphi\rangle = E_\varphi, \qquad \langle\psi_{E'}|H|\varphi\rangle = V_{E'}, \qquad \langle\chi_{E'}|H|\varphi\rangle = W_{E'} \tag{A.2}$$

$$\langle\psi_{E'}|H|\psi_{E'}\rangle = \langle\chi_{E'}|H|\chi_{E'}\rangle = E'\delta(E'' - E''), \qquad \langle\chi_{E''}|H|\psi_{E'}\rangle = 0. \tag{A.3}$$

It is understood that the discrete energy level E_φ lies within the continuous range of values E' and E''. The coefficients a, b_{nE} and c_{nE} are determined from the system of equations:

$$E_\varphi a + \int \mathrm{d}E' \,[V^*_{E'} b_{E'} + W^*_{E'} c_{E'}] = Ea \tag{A.4}$$

$$V_{E'} a + E' b_{E'} = E b_{E'} \tag{A.5}$$

$$W_{E'} a + E' c_{E'} = E c_{E'}. \tag{A.6}$$

After some rearrangement we get two orthogonal solutions:

$$a_1 = \frac{\sin\bar{\Delta}}{\pi(|V_E|^2 + |W_E|^2)^{1/2}} \tag{A.7}$$

$$b_{1E'} = \frac{V_{E'}}{(|V_E|^2 + |W_E|^2)^{1/2}}\left[\frac{1}{\pi}\frac{\sin\bar{\Delta}}{E - E'} - \cos\bar{\Delta}\delta(E - E')\right] \tag{A.8}$$

$$c_{1E'} = \frac{W_{E'}}{(|V_E|^2 + |W_E|^2)^{1/2}}\left[\frac{1}{\pi}\frac{\sin\bar{\Delta}}{E - E'} - \cos\bar{\Delta}\delta(E - E')\right] \tag{A.9}$$

where

$$\bar{\Delta} = -\arctan\frac{\pi(|V_E|^2 + |W_E|^2)}{E - E_\varphi - Z(E)} \qquad \text{and} \qquad Z(E) = P\int \mathrm{d}E' \,\frac{|V_{E'}|^2 + |W_{E'}|^2}{E - E'} \tag{A.10}$$

and

$$a_2 = 0 \tag{A.11}$$

$$b_{2E'} = \frac{W^*_{E'}}{(|V_E|^2 + |W_E|^2)^{1/2}}\delta(E - E') \tag{A.12}$$

$$c_{2E'} = -\frac{V^*_{E'}}{(|V_E|^2 + |W_E|^2)^{1/2}}\delta(E - E'). \tag{A.13}$$

The probability P_{tot} of transition from an initial state $|i\rangle$ to all states with energy E is:

$$P_{tot} = |\langle\Psi_{1E}|T|i\rangle|^2 + |\langle\Psi_{2E}|T|i\rangle|^2. \tag{A.14}$$

We are interested in the ratio P_{tot}/P_u, where P_u is the probability of a transition to the unperturbed continuum $|\psi_E\rangle$:

$$\frac{P_{tot}}{P_u} = \frac{|\langle\Psi_{1E}|T|i\rangle|^2}{|\langle\psi_E|T|i\rangle|^2} + \frac{|\langle\Psi_{2E}|T|i\rangle|^2}{|\langle\psi_E|T|i\rangle|^2}. \tag{A.15}$$

Taking into account that there is no transition from an initial state $|i\rangle$ to $|\chi_{E'}\rangle$ i.e.:

$$\langle\chi_{E'}|T|i\rangle = 0 \qquad \text{(this makes a distinction between (7) and (8))} \tag{A.16}$$

with (A.7)–(A.13), it is not difficult to show that:

$$\frac{|\langle\Psi_{1E}|T|i\rangle|^2}{|\langle\psi_E|T|i\rangle|^2} = \frac{|V_E|^2}{|V_E|^2 + |W_E|^2}(q\sin\bar{\Delta} - \cos\bar{\Delta})^2 = \frac{|V_E|^2}{|V_E|^2 + |W_E|^2}\frac{(q+\bar{\varepsilon})^2}{1+\bar{\varepsilon}^2} \tag{A.17}$$

$$\frac{|\langle\Psi_{2E}|T|i\rangle|^2}{|\langle\psi_E|T|i\rangle|^2} = \frac{|W_E|^2}{|V_E|^2 + |W_E|^2} \tag{A.18}$$

where q is the same as in (4) and $\bar{\varepsilon}$ is given by:

$$\bar{\varepsilon} = -\cot\bar{\Delta} = \frac{E - E_\varphi - Z(E)}{\pi(|V_E|^2 + |W_E|^2)} = \frac{E - E_\varphi - Z(E)}{\Gamma/2}. \tag{A.19}$$

Therefore, finally:

$$\frac{P_{tot}}{P_u} = \frac{\Gamma_2}{\Gamma} + \frac{\Gamma_1}{\Gamma}\frac{(q+\bar{\varepsilon})^2}{1+\bar{\varepsilon}^2} \tag{A.20}$$

where

$$\Gamma_1 = 2\pi|V_E|^2, \qquad \Gamma_2 = 2\pi|W_E|^2 \qquad \text{and} \qquad \Gamma = \Gamma_1 + \Gamma_2. \tag{A.21}$$

References

[1] Fano U 1961 *Phys. Rev.* **124** 1866
[2] Fano U and Cooper J W 1965 *Phys. Rev.* **137** 1364
[3] Hrostowski H J and Kaiser R H 1958 *J. Phys. Chem. Solids* **4** 148
[4] Onton A, Fisher P and Ramdas A K 1967 *Phys. Rev.* **163** 686
[5] Chandrasekhar H R, Ramdas A K and Rodriguez S 1976 *Phys. Rev.* B **14** 2417
[6] Watkins G and Fowler W B 1977 *Phys. Rev.* B **16** 4524
[7] Simonian A W, Sproul A B, Shi Z and Gauja E 1995 *Phys. Rev.* B **52** 5672
[8] Suezawa M, Kasuya A, Sumino K and Nishina Y 1988 *J. Phys. Soc. Japan* **57** 4021
[9] Baron R, Young M H and McGill T C 1983 *Solid State Commun.* **47** 167
[10] Chang Yia-Chung and McGill T C 1983 *Solid State Commun.* **47** 171
[11] Janzen E, Grossmann G, Stedman R and Grimmeiss H G 1985 *Phys. Rev.* B **31** 8000
[12] Cerdeira F, Fjeldly T A and Cardona M 1973 *Phys. Rev.* B **8** 4734
[13] Cerdeira F and Cardona M 1972 *Phys. Rev.* B **5** 1440
[14] Balkanski M, Jain K P, Beserman R and Jouanne M 1975 *Phys. Rev.* B **12** 4328
[15] Klein M V 1983 *Light Scattering in Solids* vol 1, ed M Cardona (Berlin: Springer) p 147
[16] Butschke J 2002 private communication
[17] Braun D, Gajić R, Kuchar F, Korntner R, Haugeneder E, Loeschner H, Butschke J, Letzkus F and Springer R 2003 *J. Vac. Sci. Technol.* B **21** 123
[18] Käsmaier R and Löschner H 2000 *SPIE Conf. on Microlithography (Santa Clara, Feb.–March 2000)*
[19] Butschke J, Ehrmann A, Höfflinger B, Irmsher M, Käsmaier R, Letzkus F, Löschner H, Mathuni J, Reuter C, Schomburg C and Springer R 1999 *Micro. Nano. Eng.* **46** 473
[20] Belitsky V I and Cardona M 1996 *Solid State Commun.* **100** 837
[21] Rousseau D L and Porto S P S 1968 *Phys. Rev. Lett.* **20** 1354
[22] Yafet Y 1980 *Phys. Rev.* B **21** 5023
[23] Kireev P S 1978 *Semiconductor Physics* (Moscow: Mir)
[24] Klemens P G 1955 *Proc. Phys. Soc.* A **68** 1113
[25] Brüesch P 1987 *Phonons: Theory and Experiments* vol 3 (Berlin: Springer) p 89